Modified gravity away from a CDM background

Journal of Cosmology and Astroparticle Physics
An IOP and SISSA journal

Modified gravity away from a ΛCDM background

Guilherme Brando,[a] **Felipe T. Falciano,**[a,b,1] **Eric V. Linder**[c,d,2] **and Hermano E.S. Velten**[a,e,3]

[a]PPGCosmo, CCE — Universidade Federal do Espírito Santo,
zip 29075-910, Vitória, ES, Brazil
[b]CBPF — Centro Brasileiro de Pesquisas Físicas,
Xavier Sigaud st. 150, zip 22290-180, Rio de Janeiro, RJ, Brazil
[c]Berkeley Center for Cosmological Physics & Berkeley Lab, University of California,
Berkeley, CA 94720, U.S.A.
[d]Energetic Cosmos Laboratory, Nazarbayev University,
Nur-Sultan, 010000, Kazakhstan
[e]Departamento de Física, Universidade Federal de Ouro Preto (UFOP),
zip 35400-000, Ouro Preto, MG, Brazil
E-mail: gbrando@cosmo-ufes.org, ftovar@cbpf.br, evlinder@lbl.gov,
hermano.velten@ufop.edu.br

Received May 8, 2019
Revised August 5, 2019
Accepted October 29, 2019
Published November 14, 2019

Abstract. Within the effective field theory approach to cosmic acceleration, the background expansion can be specified separately from the gravitational modifications. We explore the impact of modified gravity in a background different from a cosmological constant plus cold dark matter (ΛCDM) on the stability and cosmological observables, including covariance between gravity and expansion parameters. In No Slip Gravity the more general background allows more gravitational freedom, including both positive and negative Planck mass running. We examine the effects on cosmic structure growth, as well as showing that a viable positive integrated Sachs-Wolfe effect crosscorrelation easily arises from this modified gravity theory. Using current data we constrain parameters with a Monte Carlo analysis, finding a bound on the running $|\alpha_{M,\max}| \lesssim 0.03$ (95% CL) for the adopted form at all cosmic times. We provide the modified `hi_class` code publicly on GitHub, now enabling computation and inclusion of the redshift space distortion observable $f\sigma_8$ as well as the No Slip Gravity modifications.

Keywords: modified gravity, cosmological parameters from CMBR, cosmological parameters from LSS, dark energy theory

ArXiv ePrint: 1904.12903

[1]https://orcid.org/0000-0003-2263-1252.
[2]https://orcid.org/0000-0001-5536-9241.
[3]https://orcid.org/0000-0002-5155-7998.

https://doi.org/10.1088/1475-7516/2019/11/018

JCAP11(2019)018

Contents

1 Introduction 1

2 Gravity in a non-ΛCDM background 2

3 No Slip Gravity 3

4 Effects on cosmic growth 6

5 Lensing potential and ISW effect 8

6 Cosmology and gravity constraints 10

7 Conclusions 14

A Variation of a_t and τ 17

1 Introduction

Cosmic acceleration arises from an unknown physical origin but leaves concrete signatures in cosmic distances, growth of structure, light propagation and lensing, and cosmic microwave background (CMB) anisotropies. Careful investigation of all of these can provide insight into whether the effects are wholly due to a change in the cosmic expansion rate or also modification of the strength of gravity.

The background expansion in modified gravity theories, however, tends to be chosen as that of a cosmological constant plus cold dark matter (ΛCDM), or solved for only in the simplest viable models, such as $f(R)$, where it lies very close to ΛCDM. However, the expansion rate is a function to be specified in the theory, just as the perturbative effective field theory or property functions are [1–5]. One can also choose to work from a given Lagrangian and compute expansion and perturbations together, though one has then to check that the expansion describes the data. We follow the common path of specifying the expansion separately to ensure it is viable. Here we examine the implications of allowing background cosmologies away from ΛCDM, as well as modified gravity, and their interplay.

Of particular interest is how this affects cosmic growth observables, which depend both on the expansion rate and strength of gravity, and the crosscorrelation of perturbed quantities, such as CMB temperature anisotropies from the integrated Sachs-Wolfe (ISW) effect and galaxy clustering density. Indeed, some theories have been ruled out due to possessing an anticorrelation for this, rather than the observed positive correlation. Theories can also be discarded ab initio if they are unstable, but a non-ΛCDM background offers extra possibilities for stabilizing some theories.

The range of allowed effective theories is large, even with the tensor sector constrained to have the speed of gravitational waves equal to the speed of light. Therefore we consider particular connections between the two relevant property functions — the Planck mass running and the kinetic braiding. A specific instantiation of such a relation is No Slip Gravity [6], one of the simplest and most predictive modified gravity theories, and we use this as an exemplar for the detailed calculations.

JCAP11(2019)018

In section 2 we briefly review the property function formalism and explore the space of stable theories, also considering viability in terms of CMB observations. Section 3 examines more closely No Slip Gravity in a non-ΛCDM background, showing how the parameter space is enlarged. We investigate the impact on the cosmic structure growth rate in section 4, and the lensing potential and ISW effect in section 5. Section 6 presents a Markov Chain Monte Carlo analysis of current data and constrains background and gravity parameters simultaneously. We conclude in section 7.

2 Gravity in a non-ΛCDM background

A convenient formalism for exploring many theories of cosmic modified gravity was developed by [1], involving four property functions, and the expansion history $H(a)$. These completely characterize the theory at the linear perturbation level. While this is an impressive simplification when working with Horndeski's most general scalar-tensor gravity theory [1, 7, 8] or the effective field theory of dark energy [2–5], this still leaves five free functions of time to specify.

The detection of a binary neutron star merger with gravitational waves [9] and its electromagnetic counterparts [10, 11] provided a constraint on the speed of propagation of gravitational waves $c_T^2 = 1 + \alpha_T$, with $\alpha_T = 0$ in the most straightforward interpretation. Another property function, the kineticity α_K, has little effect on subhorizon physics and generally does not need to be specified in detail. This leaves the Planck mass running α_M and the braiding α_B, as well as the background itself, e.g. the Hubble parameter $H(a)$, where a is the cosmic expansion factor.

The arbitrariness and generality of the functional form of the $\alpha_i(a)$ functions can lead the theory to unphysical regimes. Three types of instabilities can violate the soundness of the theory: tachyon, ghost, and gradient. As pointed out, and carefully analyzed in [12], the first type of instability is less pathological and is associated with the large scale, low-k regime (where k is the Fourier mode), and is commonly not directly used in the modified gravity Boltzmann codes available in the literature, such as EFTCAMB [13, 14] and `hi_class` [15]. The other two instabilities are more severe, and must be avoided. This provides constraints on the α_i functions. For the no ghost condition, $\alpha_K + (3/2)\alpha_B^2 \geq 0$, this is readily satisfied by choosing $\alpha_K > 0$.

Avoidance of gradient instabilities corresponds to the scalar sound speed squared being nonnegative,

$$c_s^2 = \frac{1}{\alpha_K + 3\alpha_B^2/2}\left[\left(1-\frac{\alpha_B}{2}\right)\left(2\alpha_M + \alpha_B - 2\frac{H'}{H}\right) + \alpha_B' - \frac{\tilde\rho_m + \tilde p_m}{H^2}\right] \geq 0\,, \tag{2.1}$$

where a prime is a derivative with respect to $\ln a$ and a tilde denotes division by $M_\star^2(a)/M_{\rm Pl}^2$, where $M_\star^2$ is the running Planck mass squared. In terms of an effective dark energy we can write

$$c_s^2 = \frac{1}{\alpha_K + 3\alpha_B^2/2}\left[\left(1-\frac{\alpha_B}{2}\right)(2\alpha_M + \alpha_B) + \frac{(H\alpha_B)'}{H} + \frac{\rho_m}{H^2}\left(1-\frac{M_{\rm Pl}^2}{M_\star^2}\right) + \frac{\rho_{\rm de}(1+w)}{H^2}\right] \geq 0\,, \tag{2.2}$$

where w is the effective dark energy equation of state parameter. For a ΛCDM background, $1 + w = 0$.

JCAP11(2019)018

Thus a change in the background changes the stability condition. Taking the example of No Slip Gravity, where $\alpha_B = -2\alpha_M$, the stability region is

$$\frac{(\alpha_M H)'}{H} \le \frac{3}{2}\,\Omega_{\rm de}(a)\,[1+w(a)] + \frac{3}{2}\left(\Omega_m(a) - \tilde\Omega_m(a)\right)\,, \tag{2.3}$$

where $\tilde\Omega_m = \tilde\rho_m/(3H^2)$. In particular, while a ΛCDM background requires $\alpha_M \ge 0$ for stability if gravity is strengthened ($M_{\rm Pl}^2/M_\star^2 > 1$) since $H' < 0$ at all times in a normal cosmic history, in the enlarged space $\alpha_M < 0$ is also allowed.

This provides a motivation for studying non-ΛCDM backgrounds, since the enlarged parameter space may also lead to different observational characteristics. For general time dependencies $\alpha_M(a)$, $\alpha_B(a)$, and $w(a)$ there is little specific that can be said, so we will have to parametrize these functions. For the effective dark energy we adopt the common $w(a) = w_0 + w_a(1-a)$, which has been demonstrated to work for a broad class of scalar field and modified gravity theories. For $\alpha_B(a)$ we explore the class of theories where this is proportional to $\alpha_M(a)$, i.e.

$$\alpha_B(a) = -r\,\alpha_M(a)\,. \tag{2.4}$$

Such a relation holds for No Slip Gravity ($r = 2$) and $f(R)$ gravity, Brans-Dicke, and chameleon theories ($r = 1$). The ΛCDM background case was studied in [16].

Figure 1 shows the stability region for $a \le 1$ in the w_0–w_a parameter space for the example of No Slip Gravity. The ΛCDM value $(w_0, w_a) = (-1, 0)$ is stable and a significant part of the region $w_0 > -1$ is as well. There is a sharp boundary as w_0 gets appreciably smaller than -1 (roughly $w_0 < -1.026$ for the α_M parameters used; this is independent of w_a because the instability arises at late times, i.e. $a = 1$). The form of $\alpha_M(a)$ used here is the hill/valley form discussed below (a similar picture holds for the hill form of [6], also discussed below). We also indicate the mirage relation $w_a = -3.6\,(1+w_0)$ that nearly preserves the ΛCDM distance to CMB last scattering [17] and so indicates a level of observational viability.

Alternatively, figure 2 shows the stability region as we allow r to vary, but restrict the dark energy equation of state to the mirage form. (Allowing r, w_0, and w_a all to be free adds little qualitatively and diminishes the clarity of the plots.) As r gets large the stable parameter space opens up in w_0–w_a (for this hill/valley form of $\alpha_M(a)$ at least). Note that $r \to \infty$, i.e. $\alpha_M = 0$ but $\alpha_B \ne 0$, corresponds to No Run Gravity [18].

3 No Slip Gravity

For the remainder of the article we focus on No Slip Gravity, as an intriguingly minimal modification with interesting phenomenology (e.g. suppression of growth, unusual for modified gravity) and good stability. Note that even with a change in background, the no slip condition remains $\alpha_B = -2\alpha_M$.

Since eq. (2.3) allows $\alpha_M < 0$ as the right hand side can be lifted off zero, this opens a window for negative α_M at some point in its evolution.

We therefore change the hill form of [6] where

$$\begin{aligned}\alpha_M(a) &= c_M\left(1 - \tanh^2\left[\frac{\tau}{2}\ln\frac{a}{a_t}\right]\right)\\ &= \frac{c_M}{\cosh^2[(\tau/2)\ln(a/a_t)]}\\ &= \frac{4c_M\,(a/a_t)^\tau}{[(a/a_t)^\tau + 1]^2}\,,\end{aligned} \tag{3.1}$$

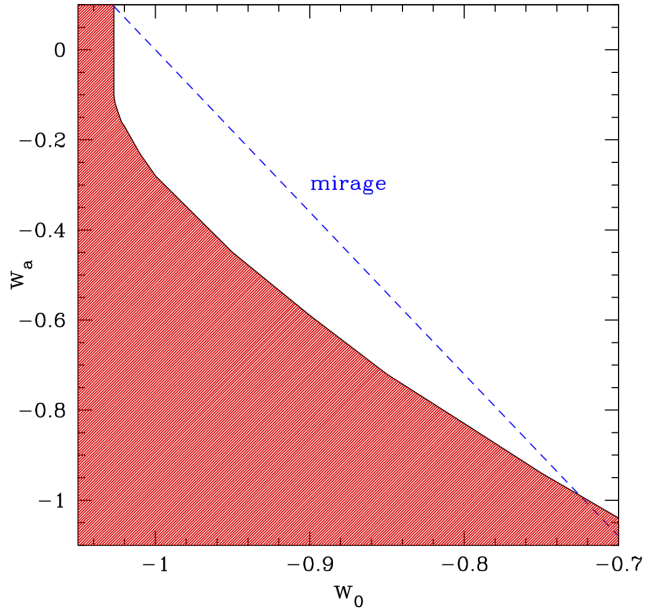

Figure 1. Stability region in the w_0–w_a plane for No Slip Gravity with the hill/valley form of $\alpha_M(a)$ with parameters $c_M = -0.05$, $\tau = 1$, and $a_t = 0.5$. Red regions indicate instability. The mirage relation $w_a = -3.6(1 + w_0)$ is plotted as the dashed blue line.

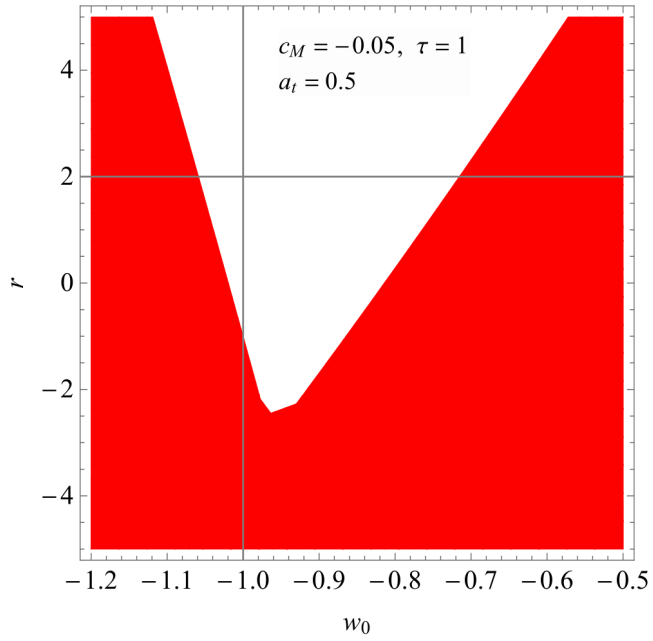

Figure 2. Stability region in the r–w_0 plane for w_a given by the mirage relation. Red regions give instability. This adopts the hill/valley form for $\alpha_M(a)$ with parameters $c_M = -0.05$, $\tau = 1$ and $a_t = 0.5$. The crosshairs center on No Slip gravity in a ΛCDM background.

JCAP11(2019)018

to allow for a negative part of $\alpha_M(a)$, i.e. a valley as well as a hill. That is, the theory changes qualitatively to permit both positive and negative Planck mass running during the evolution. The simplest modification incorporating this change without adding any further parameters we call the hill/valley form:

$$\begin{aligned}\alpha_M(a) &= c_M \frac{\tanh\left[(\tau/2)\ln(a/a_t)\right]}{\cosh^2\left[(\tau/2)\ln(a/a_t)\right]} \\ &= \frac{4c_M(a/a_t)^\tau\left[-1+(a/a_t)^\tau\right]}{\left[1+(a/a_t)^\tau\right]^3}\,.\end{aligned} \tag{3.2}$$

This illustrative form has the key characteristic of both positive and negative α_M during evolution, while retaining the flexibility to adjust the amplitude (through c_M), the breadth of the behavior (through τ), and the time of the transition (through a_t).

In the early universe $\alpha_M \approx -4c_M(a/a_t)^\tau$, so we want $\tau > 0$ to preserve general relativity at early times. (Formally one can switch the signs of τ and c_M, as seen in the first equation above, and get the same results; we take the $\tau > 0$ branch.) The function then dips into a valley / rises to a hill for $c_M > 0$ / $c_M < 0$. At late times, in the far future $a \gg a_t$, the running vanishes as $(a/a_t)^{-\tau}$. This is as expected for a de Sitter asymptote but not required for $w \neq -1$ backgrounds. However, we only apply this form to past history, $a \leq 1$, where there are observational constraints. The parameters are c_M, related to the amplitude, a_t is the scale factor of the transition between valley and hill (with $\alpha_M(a_t) = 0$), and τ measures the rapidity of the transition. Note that unlike the hill form, c_M is not the maximum amplitude; rather, the extreme (maximum and minimum) amplitudes are

$$\alpha_{M,\rm ext} = c_M\,\frac{10\pm 6\sqrt{3}}{27\pm 15\sqrt{3}} \approx \pm 0.385\,c_M\,. \tag{3.3}$$

The depth of the valley and height of the hill agree, and these occur symmetrically around a_t, with

$$a_{\rm max} = a_t\,(2+\sqrt{3})^{1/\tau} = \frac{a_t^2}{a_{\rm min}}\,. \tag{3.4}$$

For $\tau = 1$ we have $a_{\rm max} = 3.73a_t$, $a_{\rm min} = 0.27a_t$.

From $\alpha_M(a)$ one derives the Planck mass squared $M_\star^2$ through

$$\frac{M_\star^2}{M_{\rm Pl}^2} = e^{\int_0^a da'/a'\,\alpha_M(a')}\,. \tag{3.5}$$

For the hill/valley form this becomes

$$\frac{M_\star^2}{M_{\rm Pl}^2} = \exp\left[\frac{-4(c_M/\tau)(a/a_t)^\tau}{\left[1+(a/a_t)^\tau\right]^2}\right]\,. \tag{3.6}$$

This smoothly evolves from 1 in the early universe to an extremum at $a = a_t$ with $M_\star^2(a_t)/M_{\rm Pl}^2 = e^{-c_M/\tau}$ and then back to 1 in the far future.

Note that in No Slip Gravity the modified gravitational strengths in the matter and relativistic particle (light) Poisson equations are

$$G_{\rm eff} \equiv G_{\rm matter} = G_{\rm light} = \frac{M_{\rm Pl}^2}{M_\star^2}\,. \tag{3.7}$$

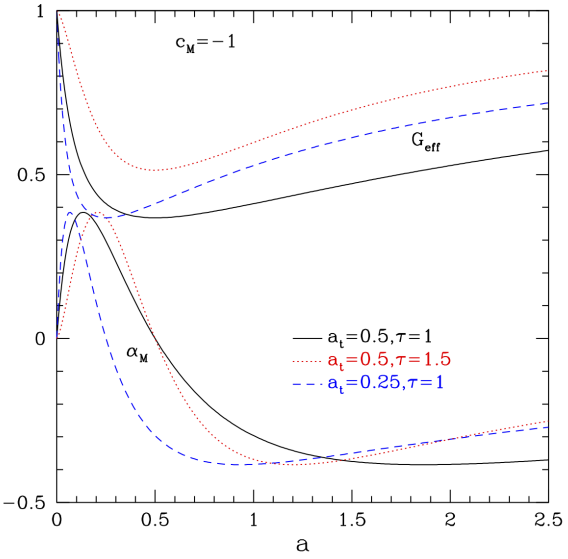

Figure 3. Curves of $G_{\rm eff}$ and α_M for the hill/valley form are shown for different values of τ and a_t, with $c_M = -1$. Positive c_M reflects α_M about 0, so hills become valleys, and inverts $G_{\rm eff}$, so values less than one become greater than one.

Whether $M_\star^2$ grows initially (weaker gravity) or diminishes (stronger gravity) depends on the sign of c_M. Stability requires $\alpha_M > 0$ in the early universe and so we must have $c_M < 0$. Thus the interesting feature of weaker gravitational strength from No Slip Gravity holds even in a non-ΛCDM background.

Figure 3 shows $\alpha_M(a)$ and $G_{\rm eff}(a)$ for different values of the hill/valley parameters. Changing a_t affects when α_M crosses zero, i.e. the transition time between the hill and valley. Increasing τ steepens the transition, moving the minimum and maximum values of α_M closer to the zero crossing. The amplitude of α_M is governed by c_M, scaling linearly with it. Inverting the sign of c_M would change hills to valleys and vice versa. For $G_{\rm eff}$, we see that indeed for $c_M < 0$ gravity is weakened, where unity corresponds to the gravitational strength being Newton's constant. The maximum weakening occurs at a_t. Since $G_{\rm eff}$ returns to unity for scale factors $a \gg a_t$, then smaller a_t means $G_{\rm eff}$ deviates from general relativity for a shorter time. Increasing τ again squeezes the transition, but also affects the maximum amplitude. Recall from eq. (3.6) that the maximum deviation is $G_{\rm eff,max} = e^{c_M/\tau}$. Increasing c_M increases the amplitude, exponentially.

For illustrative purposes, the plots in the next two sections will fix $a_t = 0.5$ and $\tau = 1$ — values near the edge of the eventual 68% confidence limit joint posterior — to more clearly show the effects of the modified gravity on observables. When we carry out Monte Carlo constraint analysis in section 6 we will show the impact of fixing a_t and τ vs fitting for $\{c_M, a_t, \tau\}$ simultaneously.

4 Effects on cosmic growth

Changes to the strength of gravity, $G_{\rm eff}$, will directly affect the growth of large scale structure in the universe. This can be measured through galaxy redshift surveys through redshift space distortions caused by the velocities due to gravitational clustering, in the form of the

JCAP11(2019)018

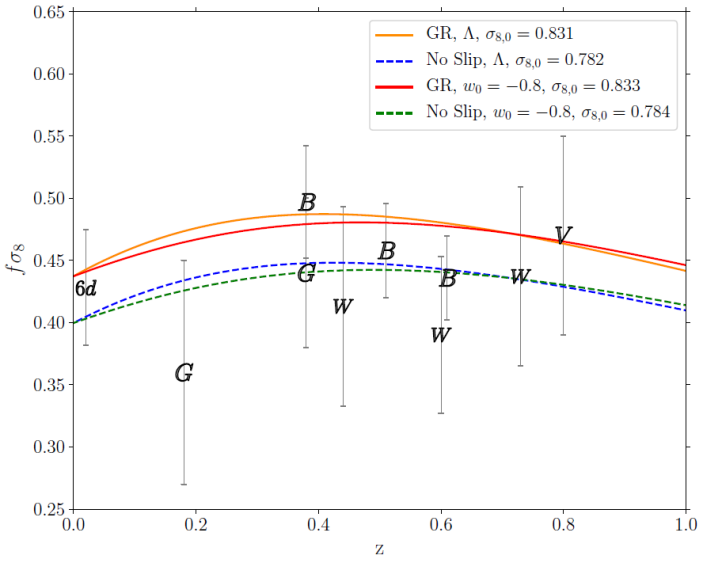

Figure 4. The redshift space distortion observable $f\sigma_8$, basically the growth rate history, is plotted for ΛCDM and for mirage dark energy with present equation of state parameter w_0, in general relativity (GR) and in No Slip Gravity with $c_M = -0.05$, $a_t = 0.5$, $\tau = 1$. All curves have fixed $\Omega_{m,0} = 0.314$ and the same initial conditions, and the derived values of $\sigma_{8,0}$ are indicated in the legend. Galaxy redshift survey data points are shown with their error bars. Note that No Slip Gravity suppresses growth, unlike many modified gravity theories, bringing the theory into better agreement with this growth data.

cosmological parameter combination $f\sigma_8(a)$. Here f is the logarithmic growth rate and σ_8 is the mass fluctuation amplitude.

For various cosmological backgrounds, i.e. expansion histories described by matter plus dark energy with a mirage equation of state, we solve numerically the subhorizon linear density perturbation growth equation with various modified gravitational strengths $G_{\rm eff}$. The solutions for the redshift space distortion (RSD) parameter $f\sigma_8(a)$ of the growth rate history are compared to the equivalent result for the same background but with general relativity, and to current observational data.

Figure 4 shows the results. The observational data points come from the galaxy redshift surveys of 6dFGRS [19], GAMA [20], BOSS [21], WiggleZ [22], and VIPERS [23]. Indeed No Slip Gravity, even in the hill/valley form where α_M can be both positive and negative during its evolution, suppresses growth relative to the general relativity with the same background expansion. This characteristic, rare for modified gravity theories, gives an improved fit to the RSD data for the same background. (To be absolutely proper, one should reanalyze the galaxy clustering data within the theory to be tested but this is beyond the scope of this paper and at the level of current data precision and small deviations from GR ΛCDM this should not be a large effect.)

We also see that the mirage dark energy models, even with an equation of state today as far from a cosmological constant as $w_0 = -0.8$, have quite similar growth histories as in the corresponding ΛCDM model of the same gravitational theory, i.e. general relativity or No Slip Gravity. This is one of the useful properties of the mirage models, even in the nonlinear power spectrum, as highlighted in [17, 24].

JCAP11(2019)018

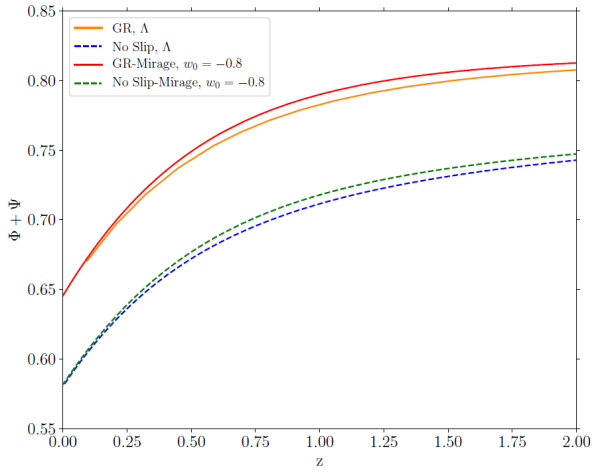

Figure 5. The Weyl lensing potential, in CLASS code units, is plotted for ΛCDM and for mirage dark energy with present equation of state parameter w_0, in general relativity (GR) and in No Slip Gravity with $c_M = -0.05$, $a_t = 0.5$, $\tau = 1$. The weakened gravity in No Slip Gravity enhances the decay of the potential, in contrast to, e.g., Galileon gravity.

5 Lensing potential and ISW effect

While we have considered the effect of modified gravity on the growth of cosmic structure, gravity also affects light propagation. That is, in addition to $G_{\rm matter}$ there is a modification of Poisson equation involving the sum of the metric potentials $\Phi + \Psi$ (often called the Weyl potential), or $G_{\rm light}$. Recall that for No Slip Gravity $G_{\rm light} = M_{\rm Pl}^2/M_\star^2$. The sum of potentials generally decays in a universe with dark energy as matter domination wanes. However, if gravity is strengthened then it could overcome this tendency and grow the potentials. This not only gives a large integrated Sachs-Wolfe (ISW) effect (proportional to $\dot\Phi + \dot\Psi$) in the CMB but can cause an anticorrelation between the ISW and the density perturbations.

Such issues are discussed in detail in [25–27], and some cubic Horndeski gravity theories indeed have a negative crosscorrelation between CMB temperature perturbations and galaxy density perturbations, C_ℓ^{Tg}. This conflicts with the prediction of ΛCDM, and data, and is a strong indicator against such theories. (We note, however, that we have verified that No Run Gravity [18], a subclass of cubic Horndeski gravity, and with a strengthening of gravity, still does have a positive crosscorrelation.)

Since No Slip Gravity weakens gravity, suppressing growth, we expect the Weyl potential to decay (i.e. weaker gravitational lensing). Figure 5 confirms this. The lensing potential in No Slip Gravity is suppressed relative to general relativity for the same background. (Note that at high redshift the curves approach the general relativity behavior.) One can use the same analytic calculation as in [28] to approximate the degree of suppression. Note that, as for growth, the mirage models act in light propagation quite similarly to the ΛCDM model they were designed to mimic in CMB distance to last scattering.

Given the preservation of the characteristic of a decaying lensing potential as in ΛCDM, we might expect a positive temperature-density crosscorrelation at large angles (low multipoles l) where the ISW effect dominates. Let us calculate this in detail. We will follow closely the procedure outlined in [26], to compute the cross correlation between the CMB

JCAP11(2019)018

temperature and a galaxy survey. First we must calculate

$$C_l^{Tg} = 4\pi \int \frac{\mathrm{d}k}{k} \Delta_l^{ISW}(k) \Delta_l^{g}(k) \mathcal{P}_{\mathcal{R}}(k)\,, \tag{5.1}$$

where $\mathcal{P}_{\mathcal{R}}$ is the power spectrum of the primordial curvature perturbations ($\mathcal{R}(\mathbf{k})$), and Δ_l^{ISW} and Δ_l^{g} are the transfer functions for the ISW effect and for the galaxies. The first is given by

$$\Delta_l^{\mathrm{ISW}} = \int_{\eta_*}^{\eta_0} \mathrm{d}\eta\, (\Phi' + \Psi') j_l\,, \tag{5.2}$$

where η_* and η_0 are the conformal time at recombination and today, respectively, and a prime here denotes a derivative with respect to η. The transfer functions depend on the modified gravity theory being considered and are calculated through the perturbation equations, which are solved numerically by `hi_class`.

For computations in which source number counts are present, the relevant transfer function is given as

$$\Delta_l^{g} \approx \Delta_l^{\mathrm{Den}_i} + \dots\,, \tag{5.3}$$

where the dots represent other contributions such as redshift-space distortions, lensing, polarization, and contributions suppressed by H/k in subhorizon scales [26]. The explicit form of $\Delta_l^{\mathrm{Den}_i}$ is

$$\Delta_l^{\mathrm{Den}_i} = \int_0^{\eta_0} \mathrm{d}\eta\, W_i b_g(\eta) \delta(\eta, k) j_l\,, \tag{5.4}$$

where $\delta(\eta, k)$ is the density perturbation at the Fourier mode k, $j_l = j_l(k(\eta_0 - \eta))$ is a Bessel function, and W_i is a window function, discussed below. To be consistent with `hi_class` all transfer functions are normalized to the value of the curvature perturbation at some time $k\eta_{\mathrm{ini}} \ll 1$, e.g. $\delta(\eta, k) = \delta(\eta, \mathbf{k})/\mathcal{R}(\eta_{\mathrm{ini}}, \mathbf{k})$.

For a galaxy sample we use the NVSS survey [29], which covers the sky north of -40 deg declination in one band. This is a large area, fairly deep survey with good overlap with the CMB ISW kernel. The selection function W_i is given by the observed number of sources per redshift, dN/dz, and we use a constant bias factor for each redshift bin. The survey selection function is given by [30] as

$$\left[b_g(z) \frac{\mathrm{d}N}{\mathrm{d}z} \right]_{\mathrm{NVSS}} = b_{\mathrm{eff}} \frac{\alpha^{\alpha+1}}{z_0^{\alpha+1}\Gamma(\alpha)} z^{\alpha} e^{-\alpha z/z_0}\,, \tag{5.5}$$

with $b_{\mathrm{eff}} = 1.98$, $z_0 = 0.79$, $\alpha = 1.18$, and Γ the gamma function.

We modified `hi_class` in order to implement (5.5) in a specific subroutine of the `transfer` module. Figure 6 shows the results. We see that indeed No Slip Gravity gives a positive ISW crosscorrelation, in agreement with the ΛCDM case, and observational data. However, without a proper calibration of the bias factor for the NVSS survey in No Slip Gravity with this background, as done in [26] for the Galileon model, we cannot investigate in quantitative detail a likelihood analysis of the ISW data. This is left for future work. The calibration of the bias would affect the height and position of the hill present for $\ell < 20$. Note that on those large scales there is also an influence of the value chosen for the α_K parameter. We have investigated this and find that for $\alpha_K = 0.1$ the effect is less than 0.2% for $\ell > 20$, rising to 0.5% for the lowest ℓ (relative to the corresponding case with $\alpha_K = 10^{-4}$). Given the size of the uncertainties in the data (including cosmic variance), this is a negligible effect.

JCAP11(2019)018

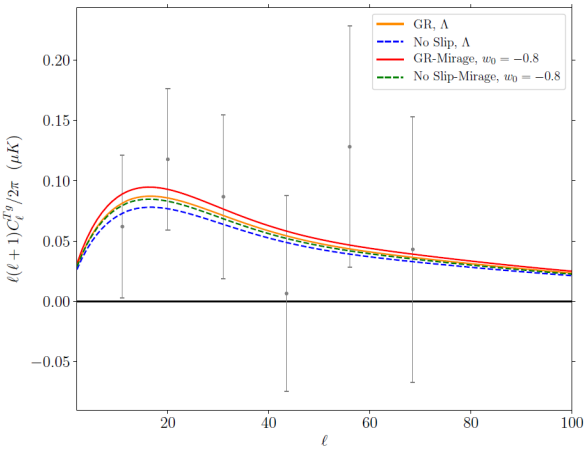

Figure 6. The ISW-galaxy crosscorrelation C_ℓ^{Tg} is plotted for ΛCDM and for mirage dark energy with present equation of state parameter w_0, in general relativity (GR) and in No Slip Gravity with $c_M = -0.05$, $a_t = 0.5$, $\tau = 1$. The data points come from the NVSS survey, as extracted from [30]. We see that, indeed, No Slip Gravity gives a positive crosscorrelation.

6 Cosmology and gravity constraints

Having explored the impact of modified gravity in a non-ΛCDM background on both growth of structure and light propagation we now proceed to perform a Markov Chain Monte Carlo (MCMC) analysis of our model using MontePython [31, 32]. We fit over the standard cosmological parameters plus some additional effective dark energy and modified gravity ones: w_0 and w_a for the background and c_M, a_t, and τ for modified gravity. We do not apply the mirage relation between w_0 and w_a, but we will find that it gives a reasonable fit to the MCMC joint confidence contour (also see figure 2 of [33]). In one case we fix $a_t = 0.5$, $\tau = 1$ as fiducial values, for reasons given in section 3, but we also allow them to vary in another case. The sum of the masses of the neutrinos (one massive and two massless) is fixed to 0.06 eV. On the extra parameters we use flat priors of $w_0 \in [-1.2, 0]$, $w_a \in [-1, 0.5]$, and $c_M \in [-0.1, 0]$. When varying the modified gravity transition parameters we use $a_t \in [0.1, 1]$ and $\tau \in [0.33, 2.19]$ from stability and observational considerations. These priors are informed by the stability analysis in appendix A.

For data sets we use CMB (Planck *TTTEEE* [34] and lensing [35]), BAO (BOSS DR12 [21], SDSS DR7 MGS [36], 6dFGS [19]), RSD (BOSS DR12 [21]), and supernovae (JLA [37]). Note that we added to `hi_class` the capability to compute the redshift space distortion observable $f\sigma_8$, which it previously lacked, and included this in MCMC likelihood evaluation for No Slip modified gravity. The modified code is publicly accessible at https://github.com/gbrandool/hi_class_public.

All the parameter constraints were extracted using the Gelman-Rubin convergence diagnostic R, with a convergence criterion of $R - 1 < 0.01$ [38]. The derived constraints for the fixed a_t and τ case are given in table 1 and the triangle plot in figure 7.

The mass fluctuation amplitude σ_8 is lower than in the Planck analysis within general relativity, due to the suppression of growth by No Slip Gravity, as presaged in figure 4. This could put it in better agreement with weak lensing measurements [39–43] (but see [44]), which are not included in this analysis. (Note the discussion in section 4 regarding formally needing to reanalyze data within the new theory.) The amplitude of the Planck mass running α_M,

JCAP11(2019)018

Param	best-fit	mean$\pm\sigma$	95% lower	95% upper
$10^2\omega_b$	2.234	$2.225^{+0.015}_{-0.016}$	2.194	2.257
$\omega_{\rm cdm}$	0.1193	$0.1194^{+0.0014}_{-0.0014}$	0.1167	0.1222
H_0	67.75	$66.59^{+1.1}_{-0.82}$	64.63	68.42
$10^9 A_s$	2.163	$2.208^{+0.058}_{-0.067}$	2.085	2.336
n_s	0.9647	$0.966^{+0.0046}_{-0.0046}$	0.9568	0.9753
$\tau_{\rm reio}$	0.06993	$0.08^{+0.014}_{-0.016}$	0.05055	0.1101
c_M	-0.005683	$-0.01252^{+0.013}_{-0.0032}$	-0.02988	0.0
w_0	-0.9953	$-0.9407^{+0.023}_{-0.064}$	-1.015	-0.8363
w_a	-0.03216	$-0.1123^{+0.19}_{-0.14}$	-0.4807	0.2184
σ_8	0.816	$0.8095^{+0.012}_{-0.011}$	0.7864	0.8323

Table 1. Results of the MCMC analysis for various cosmological and gravity parameters, for the case with $a_t = 0.5$ and $\tau = 1$ fixed.

Param	best-fit	mean$\pm\sigma$	95% lower	95% upper
$10^2\omega_b$	2.227	$2.225^{+0.016}_{-0.016}$	2.193	2.257
$\omega_{\rm cdm}$	0.119	$0.1195^{+0.0014}_{-0.0014}$	0.1167	0.1224
H_0	67.38	$66.97^{+1.1}_{-1.2}$	64.62	69.3
$10^9 A_s$	2.156	$2.193^{+0.056}_{-0.063}$	2.073	2.314
n_s	0.9662	$0.9656^{+0.0048}_{-0.0048}$	0.9561	0.9749
$\tau_{\rm reio}$	0.06865	$0.0764^{+0.014}_{-0.015}$	0.0479	0.106
c_M	-0.004449	$-0.0322^{+0.032}_{-0.009}$	-0.07995	0.0
a_t	0.275	$0.676^{+0.32}_{-0.094}$	0.2615	1.0
τ	1.446	$1.631^{+0.56}_{-0.15}$	0.8304	2.19
w_0	-0.9808	$-0.9358^{+0.039}_{-0.073}$	-1.04	-0.7972
w_a	-0.04176	$-0.188^{+0.29}_{-0.17}$	-0.7417	0.2638
σ_8	0.814	$0.8141^{+0.013}_{-0.014}$	0.7875	0.8416

Table 2. Results of the MCMC analysis for various cosmological and gravity parameters, for the case with a_t and τ varying.

in terms of c_M, is restricted at the couple of percent level ($c_M > -0.03$ at 95% CL), but this can still have a discernible effect on growth of structure and lensing. However general relativity ($c_M = 0$) is within the 95% confidence level. Again note the one sided distribution due to stability considerations.

JCAP11(2019)018

Param	best-fit	mean$\pm\sigma$	95% lower	95% upper
$10^{-2}\omega_b$	2.229	$2.225^{+0.015}_{-0.016}$	2.194	2.256
$\omega_{\rm cdm}$	0.1191	$0.1195^{+0.0013}_{-0.0014}$	0.1168	0.1223
H_0	67.64	$67.43^{+0.6}_{-0.58}$	66.22	68.61
$10^9 A_s$	2.132	$2.177^{+0.057}_{-0.064}$	2.056	2.302
n_s	0.9671	$0.9656^{+0.0045}_{-0.0046}$	0.9565	0.9748
$\tau_{\rm reio}$	0.06472	$0.07305^{+0.014}_{-0.015}$	0.0436	0.1031
c_M	−0.0002385	$-0.01762^{+0.018}_{-0.0026}$	−0.0556	0.0
a_t	0.1929	$0.696^{+0.24}_{-0.18}$	0.31	1.0
τ	0.9227	$1.456^{+0.73}_{-0.22}$	0.6165	2.19
σ_8	0.8146	$0.8176^{+0.0092}_{-0.009}$	0.7995	0.836

Table 3. Results of the MCMC analysis for various cosmological and gravity parameters, for the ΛCDM case with a_t and τ varying.

We then repeat the analysis allowing a_t and τ to vary. The results are shown in table 2 and in figure 8. Note that the a_t and τ posteriors have pulled away from the lower bounds on the priors (and the upper bounds are given by stability conditions). The exception is when c_M approaches zero — corresponding to general relativity — where a_t and τ become irrelevant, as seen from eq. (3.2). By allowing a_t and τ to vary, c_M can now assume more negative values than in the previous fixed case.

For c_M distinct from zero, larger amplitude in c_M correlates with larger τ. This follows from the Planck mass maximum being $e^{-c_M/\tau}$, and $G_{\rm eff}$ being the inverse of the Planck mass. Similarly, increasing a_t moves the maximum deviation in $G_{\rm eff}$ later, decreasing its effect, and so a_t and c_M are also correlated.

Apart from the gravity parameters, all the standard primordial cosmology parameters are consistent with the usual general relativity, ΛCDM values. We list their values in the tables, but do not show them in the triangle plots in order to make the other parameters more visible to the reader. With regard to dark energy, note the mostly one sided distribution of w_0 as required by stability considerations. The joint posterior for w_0–w_a shown in figure 11 demonstrates that mirage models come close to describing the viable models. This indicates that the CMB acoustic scale provides significant constraining power, and is also consistent with structure growth as seen in figure 4. The posterior is pulled slightly above the mirage line due to the BAO and supernovae which prefer a somewhat lower matter density at medium redshifts, and hence a more persistent dark energy ($w_0 > -1$).

Finally, we then fix to the ΛCDM background ($w_0 = -1$, $w_a = 0$) while still allowing modified gravity. The results are shown in table 3 and in figure 9. The standard cosmology parameters are little affected, and σ_8 still shows its mild suppression from the Planck GR ΛCDM value of 0.83; the GR ΛCDM value for the data sets we use is ~ 0.82 (this can also be seen roughly by slicing through the σ_8–c_M contour shown in figure 9 at the $c_M = 0$, i.e. GR, value. For the modified gravity amplitude, figure 10 compares the 1D posteriors for c_M between the three cases. They are fairly consistent with each other. When comparing the

JCAP11(2019)018

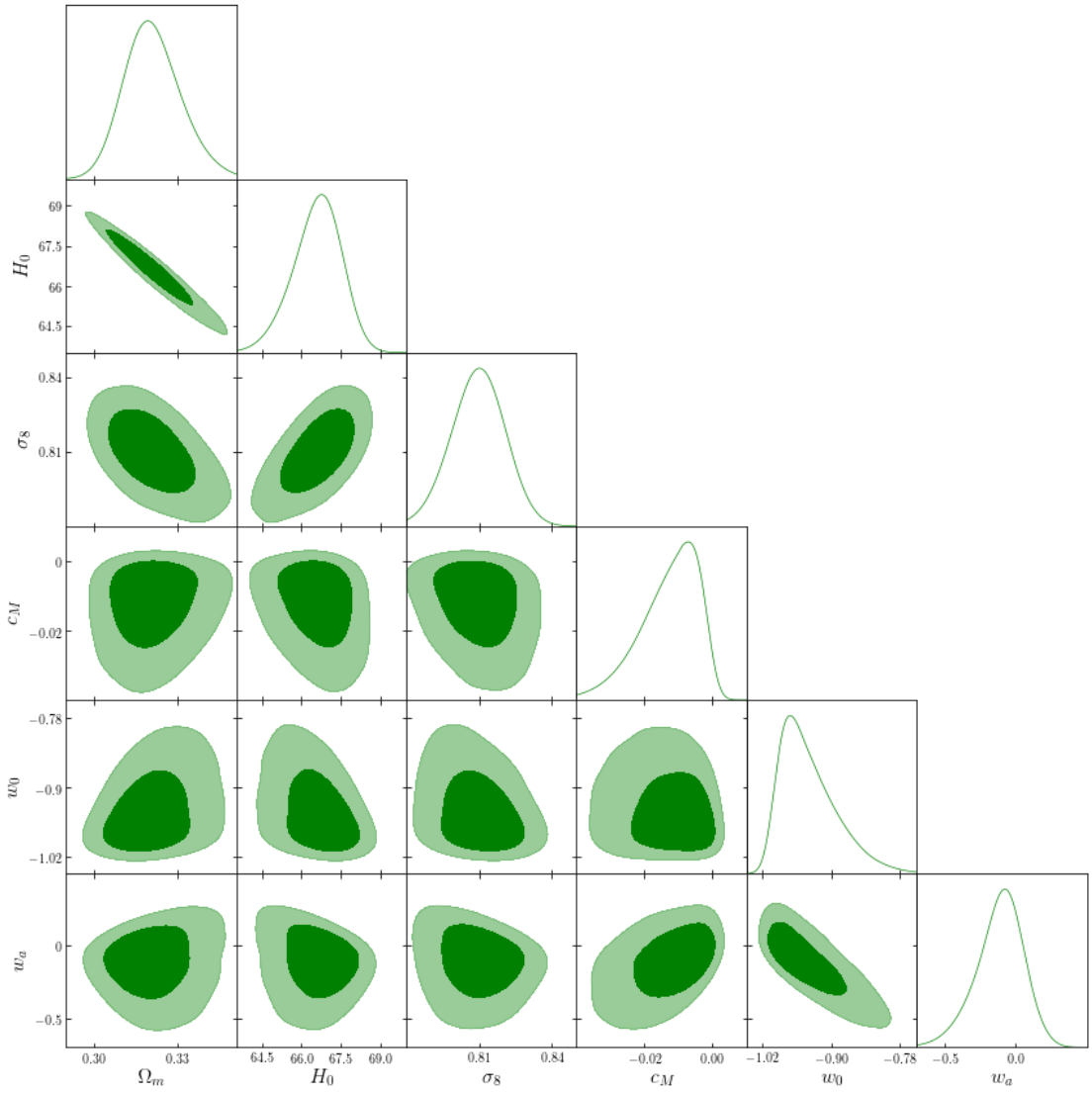

Figure 7. Triangle plot of the joint probability distributions, at 68.3% and 95.4% confidence levels, and marginalized one dimensional posteriors, for various cosmological and gravity parameters. Here $a_t = 0.5$ and $\tau = 1$ are fixed.

ΛCDM case with both w_0–w_a cases, one can see that all are consistent with general relativity at the 95% confidence level. The peak of the ΛCDM case is quite similar to the w_0–w_a case with fixed a_t and τ, while like the w_0–w_a case with varying a_t and τ there is a tail extending to more negative c_M.

The $\Delta\chi^2$ between the three cases is less than 0.4, indicating no significant preference for either allowing the background to vary (note, however, that there will be regions of model space, i.e. a_t and τ, where a ΛCDM background does not give a stable theory while a more general w_0–w_a background does) or allowing a_t and τ to vary. This is basically because all cases prefer small c_M where there is less distinction between these variations.

JCAP11(2019)018

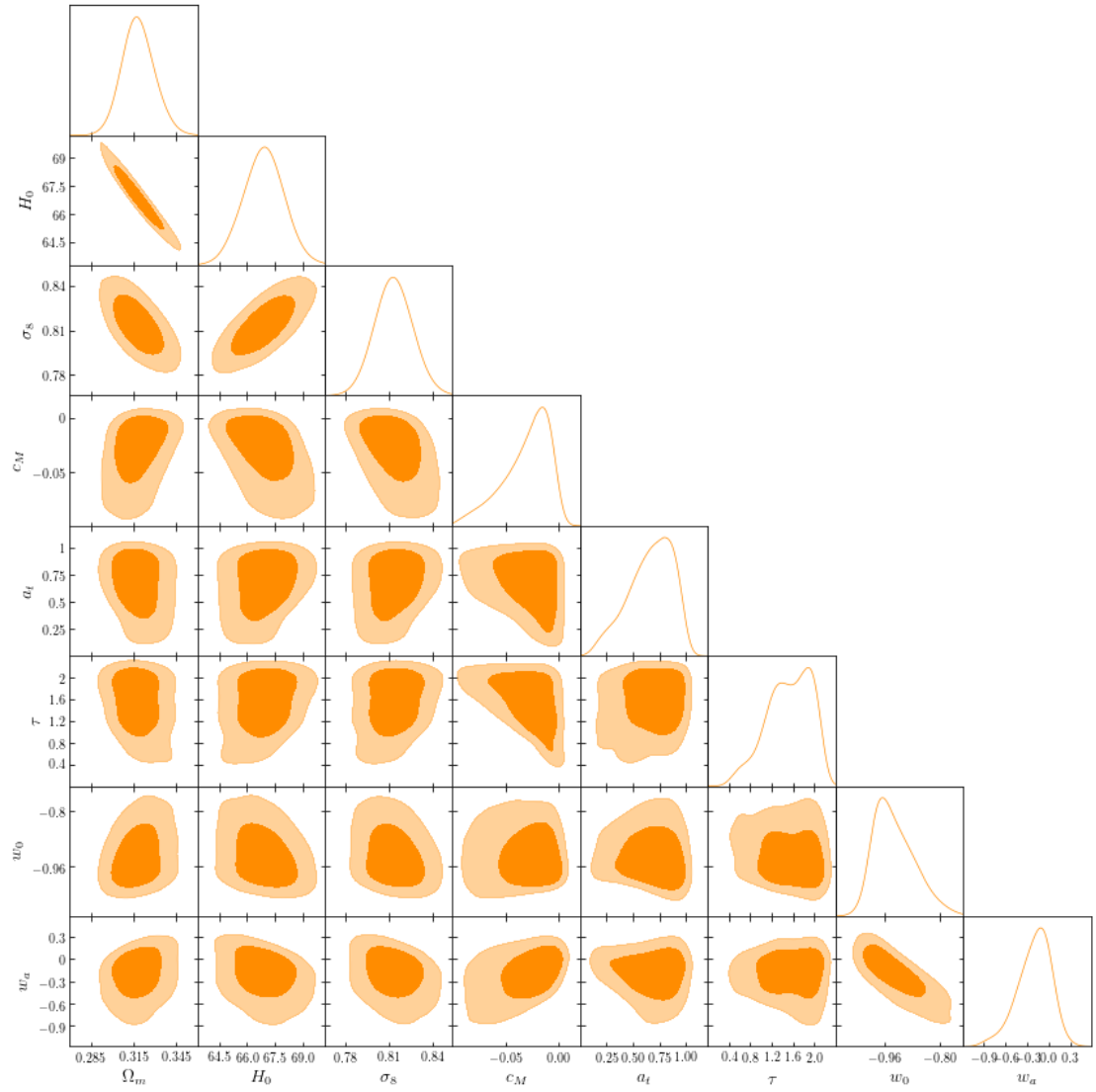

Figure 8. Triangle plot of the joint probability distributions, at 68.3% and 95.4% confidence levels, and marginalized one dimensional posteriors, for various cosmological and gravity parameters. Here a_t and τ are free to vary.

7 Conclusions

Allowing for freedom in the cosmic background history enables greater diversity of stable modified gravity models. In particular, for No Slip Gravity it broadens parameter space with $\alpha_M < 0$. To study this, we introduced a new hill-valley form for $\alpha_M(a)$ that allows both increasing and decreasing Planck mass evolution. We derived the simple analytic form for $M_\star^2$, and the effective gravitational strength $G_{\rm eff}$, plus analytic limits from stability considerations on some parameters (w_0 and τ). Beyond No Slip Gravity we also briefly explored a generalized relation between the effective field theory property functions α_B and α_M.

For the background evolution, the dark energy mirage relation gives a reasonable approximation to the preferred region of effective dark energy parameter space even within the modified gravity theory studied. This offers a way of reducing the dimension of the

JCAP11(2019)018

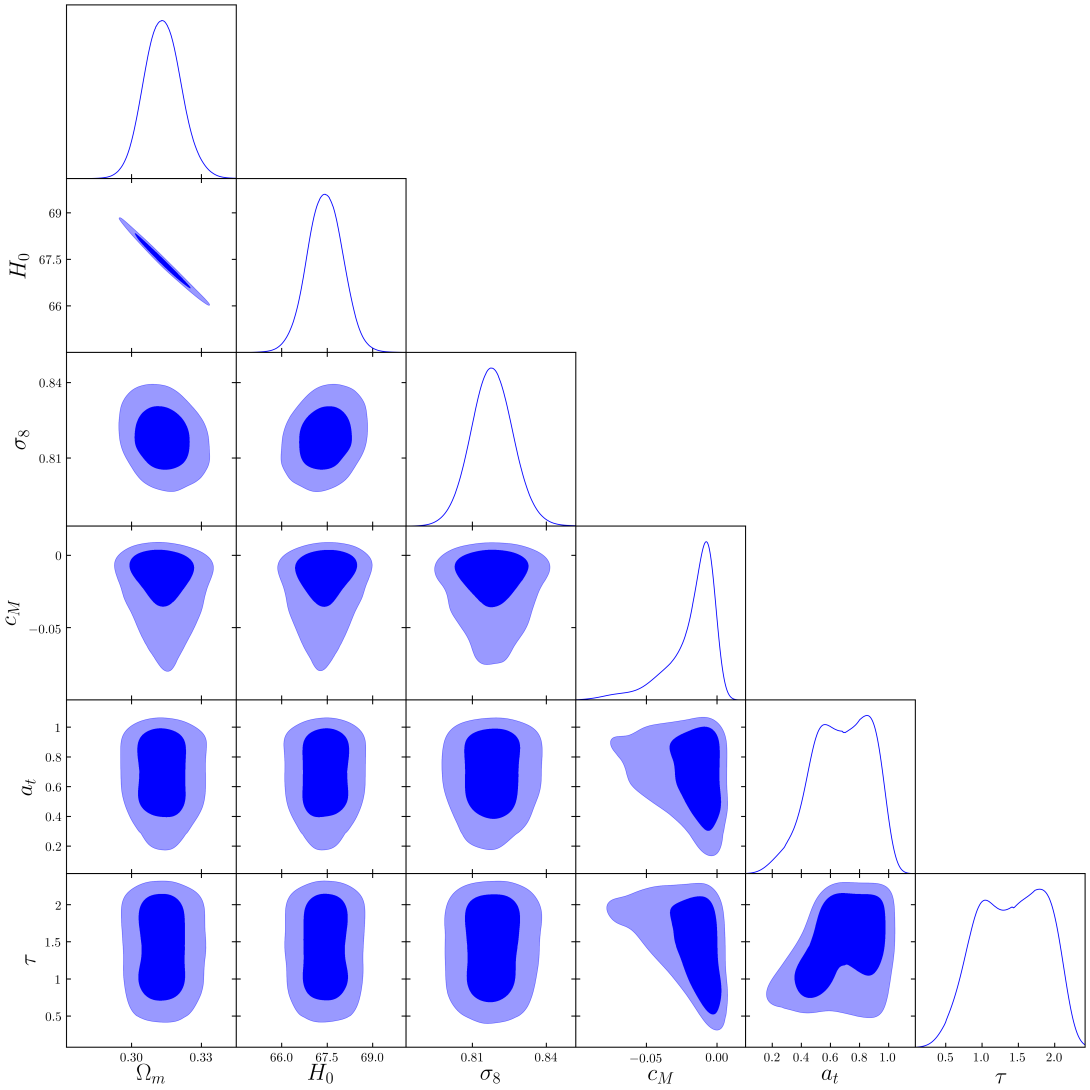

Figure 9. Triangle plot of the joint probability distributions, at 68.3% and 95.4% confidence levels, and marginalized one dimensional posteriors, for various cosmological and gravity parameters, fixing to a ΛCDM background. Here a_t and τ are free to vary.

parameter space to be fit (although we fit for the full w_0–w_a space, as well as for a ΛCDM expansion history).

No Slip Gravity is an interesting example theory in that it has a simple relation of $G_{\rm matter}$ and $G_{\rm light}$ to $M_\star^2$. Furthermore it is unusual among modified gravity theories in suppressing growth, as data mildly prefers. We extended previous analysis also to effects beyond growth, in particular $G_{\rm light}$ as well as $G_{\rm matter}$.

We studied No Slip Gravity predictions for growth of large scale structure ($f\sigma_8$), light propagation (decay of potentials and lensing), CMB, and ISW crosscorrelations. No Slip Gravity (and No Run Gravity) gives standard positive ISW-galaxy crosscorrelation — as the data prefers — unlike in some modified gravity models. We also found that an analytic approximation for lensing and ISW suppression holds for the new hill-valley model. Mirage

JCAP11(2019)018

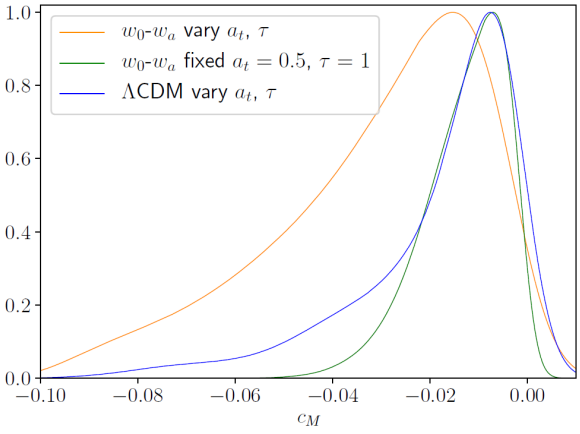

Figure 10. Marginalized one dimensional posterior comparison for the c_M parameter between the MCMC analyses performed. We can see the shift in the distribution to more negative values when τ and a_t are allowed to vary. (Note the tails to positive c_M are artifacts of the plotting and do not occur in the chains due to stability conditions.)

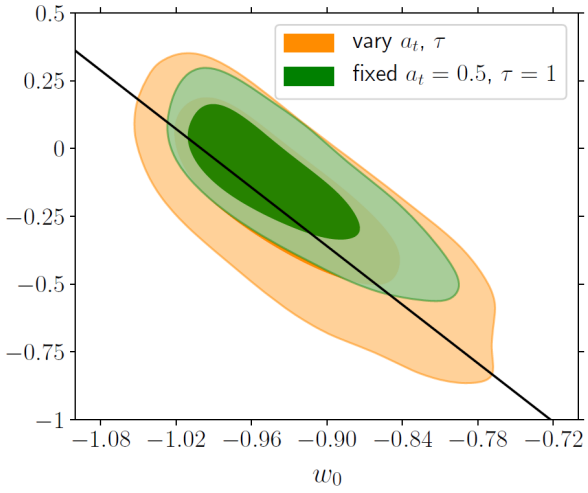

Figure 11. The joint posterior between the dark energy equation of state parameters is shown for the two analysis cases, with the mirage line $w_a = -3.6\,(1 + w_0)$ overlaid.

models were demonstrated to have similar growth histories to each other in GR, and in modified gravity, i.e. mirage dark energy with $w_0 = -0.8$ is similar to ΛCDM even in modified gravity. This holds as well with respect to similar lensing suppression.

We modified the Boltzmann code `hi_class` for this new model of No Slip Gravity (with the modified version made publicly available on GitHub at the URL give in section 6), and furthermore adapted the code to enable computation of the redshift space distortion observable $f\sigma_8$ and its application in MCMC likelihood evaluation for modified gravity.

Carrying out an MCMC analysis using current data we find the background parameters are consistent with general relativity and ΛCDM, but the modified gravity case somewhat lowers the value of σ_8, even in a ΛCDM background, easing the tension with weak lensing measurements interpreted within GR ΛCDM(taking into account the cautions of section VI where the weak lensing data analysis should be done within the new theory). Note that

JCAP11(2019)018

No Slip Gravity suppresses both structure growth and lensing deflection. For the amplitude of the modified gravity strength, $0 > c_M > -0.08$, i.e. $|\alpha_{M,\max}| < 0.03$. That is, over the entire evolution the Planck mass running cannot be too severe and so the modified gravity cannot lie too far from general relativity. In addition, general relativity lies within the 95% confidence level.

Acknowledgments

We gratefully acknowledge helpful conversations with Miguel Zumalacárregui. This work made use of the CHE cluster, managed and funded by COSMO/CBPF/MCTI, with financial support from FINEP and FAPERJ, and operating at the Javier Magnin Computing Center/CBPF. GB would like to acknowledge the State Scientific and Innovation Funding Agency of Espirito Santo (FAPES, Brazil) and the Brazilian Physical Society (SBF) through the SBF/APS PhD Exchange Program for financial support. GB would also like to thank LBL for the hospitality and financial support. FTF would like to thank the National Scientific and Technological Research Council (CNPq, Brazil) for financial support. HV would like to thank FAPES and CNPq for financial support. GB gratefully acknowledges Renan A. Oliveira and David Camarena for useful discussions in an early version of this work. This work is supported in part by the Energetic Cosmos Laboratory and by the U.S. Department of Energy, Office of Science, Office of High Energy Physics, under Award DE-SC-0007867 and contract no. DE-AC02-05CH11231.

A Variation of a_t and τ

As described in section 3, the values chosen for the transition time and width parameters, a_t and τ, of the hill/valley form for the illustrative plots were motivated by physical reasons of being close to the onset of cosmic acceleration and having the transition of order one e-fold of expansion. This also leads to an opportunity for the modified gravity to have an appreciable impact on observations. Of course in section 6 the Monte Carlo analysis scans over these parameters.

Here we show that the reasonably natural values chosen, $a_t = 0.5$ and $\tau = 1$, are not special with regard to stability considerations, i.e. not a small island in parameter space. This also motivates priors for the Monte Carlo sampling. Figure 12 shows the stability region in the τ–w_0 plane for the mirage model, fixing the other hill/valley parameters to the fiducial values: $c_M = -0.05$ and $a_t = 0.5$. Values of τ larger than $\tau_c = (3 + \sqrt{33})/4 \approx 2.19$ are ruled out by instability at early times (this value is independent of c_M and a_t); the side regions are ruled out by instability at more recent times. Figure 13 shows the corresponding diagram in the a_t–w_0 plane, with fixed $\tau = 1$. A transition occurring too early gives rise to instability at early times.

JCAP11(2019)018

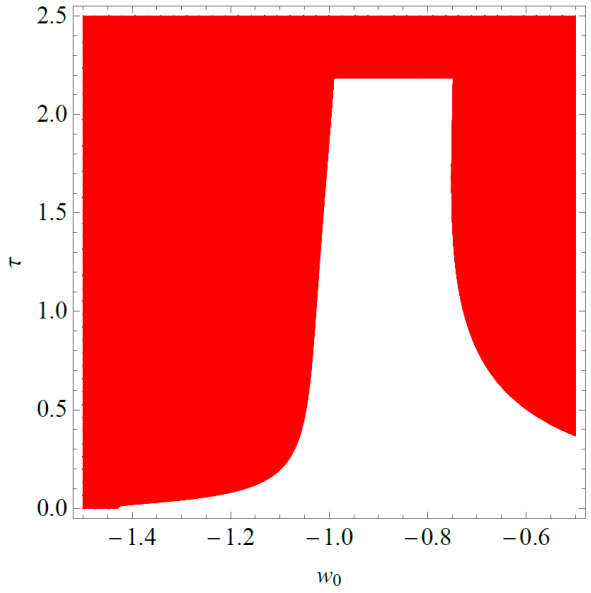

Figure 12. The stability region for the hill/valley form of α_M is shown in the τ–w_0 plane, for the mirage dark energy equation of state. The unplotted parameters are set to their fiducial values $c_M = -0.05$, $a_t = 0.5$.

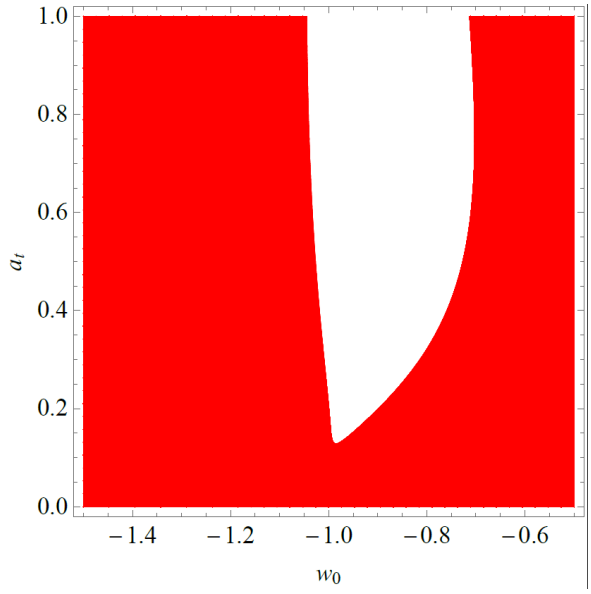

Figure 13. As Figure 12 but for the a_t–w_0 plane. The unplotted parameters are set to their fiducial values $c_M = -0.05$, $\tau = 1$.

JCAP11(2019)018

References

[1] E. Bellini and I. Sawicki, *Maximal freedom at minimum cost: linear large-scale structure in general modifications of gravity*, *JCAP* **07** (2014) 050 [arXiv:1404.3713] [INSPIRE].

[2] G. Gubitosi, F. Piazza and F. Vernizzi, *The Effective Field Theory of Dark Energy*, *JCAP* **02** (2013) 032 [arXiv:1210.0201] [INSPIRE].

[3] J.K. Bloomfield, E.E. Flanagan, M. Park and S. Watson, *Dark energy or modified gravity? An effective field theory approach*, *JCAP* **08** (2013) 010 [arXiv:1211.7054] [INSPIRE].

[4] J. Gleyzes, D. Langlois, F. Piazza and F. Vernizzi, *Essential Building Blocks of Dark Energy*, *JCAP* **08** (2013) 025 [arXiv:1304.4840] [INSPIRE].

[5] E.V. Linder, G. Sengör and S. Watson, *Is the Effective Field Theory of Dark Energy Effective?*, *JCAP* **05** (2016) 053 [arXiv:1512.06180] [INSPIRE].

[6] E.V. Linder, *No Slip Gravity*, *JCAP* **03** (2018) 005 [arXiv:1801.01503] [INSPIRE].

[7] G.W. Horndeski, *Second-order scalar-tensor field equations in a four-dimensional space*, *Int. J. Theor. Phys.* **10** (1974) 363 [INSPIRE].

[8] C. Deffayet, X. Gao, D.A. Steer and G. Zahariade, *From k-essence to generalised Galileons*, *Phys. Rev.* **D 84** (2011) 064039 [arXiv:1103.3260] [INSPIRE].

[9] LIGO Scientific and Virgo collaborations, *GW170817: Observation of Gravitational Waves from a Binary Neutron Star Inspiral*, *Phys. Rev. Lett.* **119** (2017) 161101 [arXiv:1710.05832] [INSPIRE].

[10] LIGO Scientific, Virgo, Fermi-GBM and INTEGRAL collaborations, *Gravitational Waves and Gamma-rays from a Binary Neutron Star Merger: GW170817 and GRB 170817A*, *Astrophys. J.* **848** (2017) L13 [arXiv:1710.05834] [INSPIRE].

[11] B.P. Abbott et al., *Multi-messenger Observations of a Binary Neutron Star Merger*, *Astrophys. J.* **848** (2017) L12 [arXiv:1710.05833] [INSPIRE].

[12] N. Frusciante, G. Papadomanolakis, S. Peirone and A. Silvestri, *The role of the tachyonic instability in Horndeski gravity*, *JCAP* **02** (2019) 029 [arXiv:1810.03461] [INSPIRE].

[13] B. Hu, M. Raveri, N. Frusciante and A. Silvestri, *Effective Field Theory of Cosmic Acceleration: an implementation in CAMB*, *Phys. Rev.* **D 89** (2014) 103530 [arXiv:1312.5742] [INSPIRE].

[14] M. Raveri, B. Hu, N. Frusciante and A. Silvestri, *Effective Field Theory of Cosmic Acceleration: constraining dark energy with CMB data*, *Phys. Rev.* **D 90** (2014) 043513 [arXiv:1405.1022] [INSPIRE].

[15] M. Zumalacárregui, E. Bellini, I. Sawicki, J. Lesgourgues and P.G. Ferreira, *hi_class: Horndeski in the Cosmic Linear Anisotropy Solving System*, *JCAP* **08** (2017) 019 [arXiv:1605.06102] [INSPIRE].

[16] M. Denissenya and E.V. Linder, *Gravity's Islands: Parametrizing Horndeski Stability*, *JCAP* **11** (2018) 010 [arXiv:1808.00013] [INSPIRE].

[17] E.V. Linder, *The Mirage of $w = -1$*, arXiv:0708.0024 [INSPIRE].

[18] E.V. Linder, *No Run Gravity*, *JCAP* **07** (2019) 034 [arXiv:1903.02010] [INSPIRE].

[19] F. Beutler et al., *The 6dF Galaxy Survey: $z \approx 0$ measurement of the growth rate and σ_8*, *Mon. Not. Roy. Astron. Soc.* **423** (2012) 3430 [arXiv:1204.4725] [INSPIRE].

[20] C. Blake et al., *Galaxy And Mass Assembly (GAMA): improved cosmic growth measurements using multiple tracers of large-scale structure*, *Mon. Not. Roy. Astron. Soc.* **436** (2013) 3089 [arXiv:1309.5556] [INSPIRE].

JCAP11(2019)018

[21] BOSS collaboration, *The clustering of galaxies in the completed SDSS-III Baryon Oscillation Spectroscopic Survey: cosmological analysis of the DR12 galaxy sample*, *Mon. Not. Roy. Astron. Soc.* **470** (2017) 2617 [arXiv:1607.03155] [INSPIRE].

[22] C. Blake et al., *The WiggleZ Dark Energy Survey: Joint measurements of the expansion and growth history at $z < 1$*, *Mon. Not. Roy. Astron. Soc.* **425** (2012) 405 [arXiv:1204.3674] [INSPIRE].

[23] S. de la Torre et al., *The VIMOS Public Extragalactic Redshift Survey (VIPERS). Galaxy clustering and redshift-space distortions at $z = 0.8$ in the first data release*, *Astron. Astrophys.* **557** (2013) A54 [arXiv:1303.2622] [INSPIRE].

[24] M.J. Francis, G.F. Lewis and E.V. Linder, *Power Spectra to 1% Accuracy between Dynamical Dark Energy Cosmologies*, *Mon. Not. Roy. Astron. Soc.* **380** (2007) 1079 [arXiv:0704.0312] [INSPIRE].

[25] J. Renk, M. Zumalacárregui and F. Montanari, *Gravity at the horizon: on relativistic effects, CMB-LSS correlations and ultra-large scales in Horndeski's theory*, *JCAP* **07** (2016) 040 [arXiv:1604.03487] [INSPIRE].

[26] J. Renk, M. Zumalacárregui, F. Montanari and A. Barreira, *Galileon gravity in light of ISW, CMB, BAO and H_0 data*, *JCAP* **10** (2017) 020 [arXiv:1707.02263] [INSPIRE].

[27] J. Noller and A. Nicola, *Cosmological parameter constraints for Horndeski scalar-tensor gravity*, *Phys. Rev.* **D 99** (2019) 103502 [arXiv:1811.12928] [INSPIRE].

[28] M. Brush, E.V. Linder and M. Zumalacárregui, *No Slip CMB*, *JCAP* **01** (2019) 029 [arXiv:1810.12337] [INSPIRE].

[29] http://www.cv.nrao.edu/nvss/.

[30] S. Ho, C. Hirata, N. Padmanabhan, U. Seljak and N. Bahcall, *Correlation of CMB with large-scale structure: I. ISW Tomography and Cosmological Implications*, *Phys. Rev.* **D 78** (2008) 043519 [arXiv:0801.0642] [INSPIRE].

[31] B. Audren, J. Lesgourgues, K. Benabed and S. Prunet, *Conservative Constraints on Early Cosmology: an illustration of the Monte Python cosmological parameter inference code*, *JCAP* **02** (2013) 001 [arXiv:1210.7183] [INSPIRE].

[32] T. Brinckmann and J. Lesgourgues, *MontePython 3: boosted MCMC sampler and other features*, arXiv:1804.07261 [INSPIRE].

[33] E. Di Valentino, A. Melchiorri, E.V. Linder and J. Silk, *Constraining Dark Energy Dynamics in Extended Parameter Space*, *Phys. Rev.* **D 96** (2017) 023523 [arXiv:1704.00762] [INSPIRE].

[34] PLANCK collaboration, *Planck 2015 results. XI. CMB power spectra, likelihoods and robustness of parameters*, *Astron. Astrophys.* **594** (2016) A11 [arXiv:1507.02704] [INSPIRE].

[35] PLANCK collaboration, *Planck 2015 results. XV. Gravitational lensing*, *Astron. Astrophys.* **594** (2016) A15 [arXiv:1502.01591] [INSPIRE].

[36] A.J. Ross, L. Samushia, C. Howlett, W.J. Percival, A. Burden and M. Manera, *The clustering of the SDSS DR7 main Galaxy sample — I. A 4 per cent distance measure at $z = 0.15$*, *Mon. Not. Roy. Astron. Soc.* **449** (2015) 835 [arXiv:1409.3242] [INSPIRE].

[37] SDSS collaboration, *Improved cosmological constraints from a joint analysis of the SDSS-II and SNLS supernova samples*, *Astron. Astrophys.* **568** (2014) A22 [arXiv:1401.4064] [INSPIRE].

[38] A. Gelman and D.B. Rubin, *Inference from Iterative Simulation Using Multiple Sequences*, *Statist. Sci.* **7** (1992) 457.

[39] H. Hildebrandt et al., *KiDS-450: Cosmological parameter constraints from tomographic weak gravitational lensing*, *Mon. Not. Roy. Astron. Soc.* **465** (2017) 1454 [arXiv:1606.05338] [INSPIRE].

JCAP11(2019)018

[40] S. Joudaki et al., *KiDS-450 + 2dFLenS: Cosmological parameter constraints from weak gravitational lensing tomography and overlapping redshift-space galaxy clustering*, *Mon. Not. Roy. Astron. Soc.* **474** (2018) 4894 [arXiv:1707.06627] [INSPIRE].

[41] DES collaboration, *Dark Energy Survey year 1 results: Cosmological constraints from galaxy clustering and weak lensing*, *Phys. Rev.* **D 98** (2018) 043526 [arXiv:1708.01530] [INSPIRE].

[42] DES collaboration, *Dark Energy Survey Year 1 results: Cosmological constraints from cosmic shear*, *Phys. Rev.* **D 98** (2018) 043528 [arXiv:1708.01538] [INSPIRE].

[43] A. Amon et al., *KiDS+2dFLenS+GAMA: Testing the cosmological model with the $E_{\rm G}$ statistic*, *Mon. Not. Roy. Astron. Soc.* **479** (2018) 3422 [arXiv:1711.10999] [INSPIRE].

[44] HSC collaboration, *Cosmology from cosmic shear power spectra with Subaru Hyper Suprime-Cam first-year data*, *Publ. Astron. Soc. Jap.* **71** (2019) 43 [arXiv:1809.09148] [INSPIRE].

JCAP11(2019)018